JACS
JOURNAL OF THE AMERICAN CHEMICAL SOCIETY
Communication
pubs.acs.org/JACS

Modular and Stepwise Synthesis of a Hybrid Metal–Organic Framework for Efficient Electrocatalytic Oxygen Evolution

Jian-Qiang Shen, Pei-Qin Liao,* Dong-Dong Zhou, Chun-Ting He, Jun-Xi Wu, Wei-Xiong Zhang, Jie-Peng Zhang,* and Xiao-Ming Chen

MOE Key Laboratory of Bioinorganic and Synthetic Chemistry, School of Chemistry, Sun Yat-Sen University, Guangzhou 510275, China

Supporting Information

ABSTRACT: The paddle-wheel type cluster $Co_2(RCOO)_4(L^T)_2$ (R = substituent group, L^T = terminal ligand), possessing unusual metal coordination geometry compared with other cobalt compounds, may display high catalytic activity but is highly unstable especially in water. Here, we show that with judicious considerations of the host/guest geometries and modular synthetic strategies, the labile dicobalt clusters can be immobilized and stabilized in a metal–organic framework (MOF) as coordinative guests. The $Fe(na)_4(L^T)$ fragment in the MOF $[\{Fe_3(\mu_3\text{-}O)(bdc)_3\}_4\{Fe(na)_4(L^T)\}_3]$ (H_2bdc = 1,4-benzenedicaboxylic acid, Hna = nicotinic acid) can be removed to give $[\{Fe_3(\mu_3\text{-}O)(bdc)_3\}_4]$ with a unique framework connectivity possessing suitable distribution of open metal sites for binding the dicobalt cluster in the form of $Co_2(na)_4(L^T)_2$. After two-step, single-crystal to single-crystal, postsynthetic modifications, a thermal-, water-, and alkaline-stable MOF $[\{Fe_3(\mu_3\text{-}O)(bdc)_3\}_4\{Co_2(na)_4(L^T)_2\}_3]$ containing the desired dicobalt cluster was obtained, giving extraordinarily high electrocatalytic oxygen evolution activity in water at pH = 13 with overpotential as low as 225 mV at 10.0 mA cm^{-2}.

The oxygen evolution reaction (OER) is one of the key processes for many energy storage and conversion applications,[1,2] such as hydrogen production from water splitting,[3,4] regenerative fuel cells,[5] and rechargeable metal–air batteries.[1,6] Because of its intrinsic high kinetic barrier, OER requires efficient electrocatalysts that can work in acidic or alkaline solutions.[1,7] Cobalt-based OER catalysts, including inorganic nanoparticles[8−12] and molecular complexes,[13] have attracted extensive interest due to their relatively high activities and earth-abundance of the metal.[14−17]

Besides the well investigated applications such as adsorption, storage, separation,[18,19] and conventional catalysis,[20] metal–organic frameworks (MOFs) are emerging as potential electrocatalysts for CO_2 reduction, hydrogen evolution reaction (HER), OER, etc.[21−25] However, only a handful of examples (most are cobalt-based) have been reported for electrocatalytic OER,[26−29] because these materials are usually unstable in water especially at acidic/alkaline conditions.[30] Nevertheless, metal ions in MOFs can display some special coordination structures hardly observed in the pure inorganic materials. For example, the paddle-wheel type dinuclear metal carboxylate cluster, $M_2(RCOO)_4$ or $M_2(RCOO)_4(L^T)_2$ (M = transition metal, R = substituent group, L^T = monodentate terminal ligand such as H_2O), is a classic building block of MOF,[31] in which the square-planar or square-pyramidal coordination geometries are unstable for most metal ions, giving them relatively high adsorption affinities[32] and/or catalytic activities,[33] as well as low chemical stabilities.[30] Although many MOFs have been constructed by $M_2(RCOO)_4(H_2O)_2$ (M = Cu, Zn, Ni, Fe, Co, Mo, Cr, Ru) clusters,[31,32,34,35] they have poor stability in water.[30] So far, only one MOF structure based on the $Co_2(RCOO)_4(H_2O)_2$ cluster has been constructed by the help of a large and irremovable template, because the cluster is not stable enough to support an open coordination framework.[35] General strategies for improving the stability of MOFs mainly include enhancing coordination bond strength by using ligands with high basicity (such as in metal azolate frameworks or MAFs)[27] or by using metal ions with high oxidation states (such as in Fe(III) carboxylate frameworks),[36] and protecting coordination bonds from nucleophilic attack by coating with hydrophobic units.[37] However, these strategies either cannot apply to the $Co_2(RCOO)_4(H_2O)_2$ system or will reduce the reactivity of metal ions and water. Here, we report a modular synthesis strategy for stabilizing and utilizing the $Co_2(RCOO)_4(H_2O)_2$ cluster.

Among various types of MOFs, metal carboxylate frameworks (MCFs) based on $Fe_3(\mu_3\text{-}O)(RCOO)_6(L^T)_3$ clusters, such as $[Fe_3(\mu_3\text{-}O)(bdc)_3(L^T)_3]$ (H_2bdc = 1,4-benzenedicaboxylic acid) isomers with the 6-connected **acs** (MIL-88B) and **mtn-e** (MIL-101) topologies,[38,39] are famous for their high chemical stabilities.[36] When $Fe_3(\mu_3\text{-}O)(RCOO)_6(L^T)_3$ clusters are properly arranged (mainly determined by the network topology), their open metal sites (OMSs) can fix multiple monodentate guest molecules in specific configurations to promote special chemical reactions or accommodate multidentate ligand/metalloligands to form structurally decorated MOFs.[40−43] For example, the triangularly arranged OMSs in MIL-88B can enforce three monodentate unsaturated monomers to undergo [2+2+2] cyclotrimerization reactions, and the resultant tridenate ligand rigidifies the whole coordination network.[41] The hypothetical (MIL-hypo-2) isomer of $[Fe_3(\mu_3\text{-}O)(bdc)_3(L^T)_3]$ has large framework tension because its **flu-e** topology requires large distortion of the cluster. Nonetheless, the arrangement of its OMSs perfectly fits the size and

Received: November 30, 2016
Published: January 23, 2017

DOI: 10.1021/jacs.6b12353
J. Am. Chem. Soc. 2017, 139, 1778−1781

geometry of bowl-shaped tetradentate metalloligands consisting four nicotinate (na^-) ligands with a paddle-wheel type metal carboxylate core, giving structurally reinforced MOFs such as $[\{Ni_3(\mu_3\text{-}O)(bdc)_3\}_4\{Ni_2(na)_4(L^T)_2\}_3]$ (MCF-36 or **Ni_3-Ni_2**) and $[\{Fe_3(\mu_3\text{-}O)(bdc)_3\}_4\{Fe(na)_4(L^T)\}_3]$ (MCF-37 or **Fe_3-Fe**, Figures 1a and S1a). In principle, as a structural analogue of

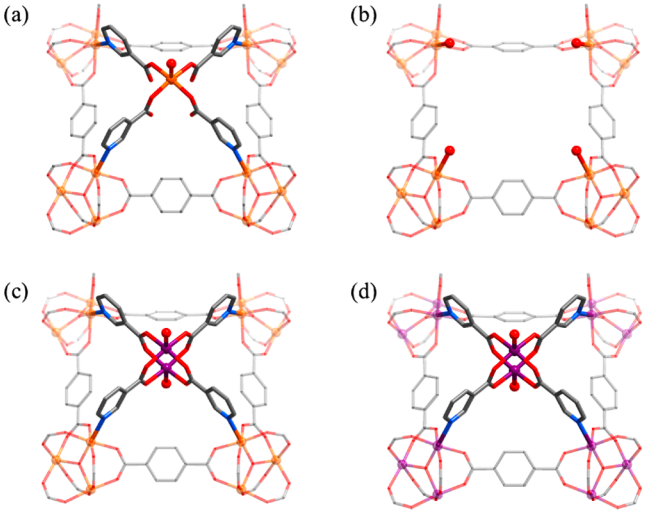

Figure 1. Key local structures of (a) **Fe_3-Fe**, (b) **Fe_3**, (c) **Fe_3-Co_2**, and (d) **Co_3-Co_2**.

$Ni_2(na)_4(L^T)_2$ and $Fe(na)_4(L^T)$, $Co_2(na)_4(L^T)_2$ should be able to cross-link the **flu-e** type $[Fe_3(\mu_3\text{-}O)(bdc)_3(L^T)_3]$ network to give a hybrid MOF $[\{Fe_3(\mu_3\text{-}O)(bdc)_3\}_4\{Co_2(na)_4(L^T)_2\}_3]$ (MCF-49 or **Fe_3-Co_2**). By virtue of the high chemical stability of the $[Fe_3(\mu_3\text{-}O)(bdc)_3(L^T)_3]$ (**Fe_3**) scaffold, the $Co_2(na)_4(L^T)_2$ (**Co_2**) cluster may be stabilized to serve as catalytic center in water.

Fe_3-Fe was obtained by solvothermal reaction of $FeCl_2$, H_2bdc, and Hna in *N*,*N*-dimethylacetamide according to our earlier report (Scheme 1).[44] Because **Fe_3** cannot be synthesized

Scheme 1. Modular and Stepwise Synthesis of Fe_3-Co_2

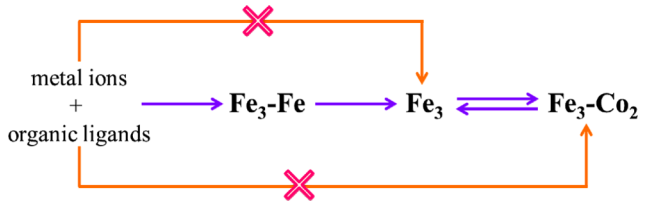

directly, we first tried to obtain **Fe_3-Co_2** by postsynthetic ion exchange of **Fe_3-Fe** with cobalt salt. Although the ion-exchange product retained the framework structure (Figure S2), inductively coupled plasma atomic emission spectroscopy (ICP-AES) showed Fe/Co molar ratios of 2.35:1, 1.26:1, and 0.92:1 after 1, 3, or 7 days (Table S1), meaning either incomplete conversion and/or undesired exchange at the **Fe_3** backbone.

Interestingly, although the powder X-ray diffraction (PXRD) pattern of **Fe_3-Fe** remains unchanged in water at pH = 1−13, its color slowly changes from dark brown to red in acidic solution, suggesting an alteration of the coordination environment of Fe ions. Indeed, the $Fe(na)_4(L^T)$ unit in **Fe_3-Fe** can be washed off by dilute HCl in a single-crystal to single-crystal manner (Table S2). Single-crystal X-ray analysis of the remained **flu-e** type $[Fe_3(\mu_3\text{-}O)(bdc)_3(L^T)_3]$ (MCF-48 or **Fe_3**) backbone, i.e., the hypothetical MOF MIL-hypo-2,[45] confirmed that the $Fe(na)_4(L^T)$ unit was replaced by four small terminal ligands (Figures 1b, S1b and Scheme 1). Mass spectrometry (MS) and nuclear magnetic resonance (NMR) spectroscopy (Figure S3) of acid-digested **Fe_3** also confirmed the complete removal of na^-. Then, crystals of **Fe_3-Co_2** were obtained by a further postsynthetic reaction of **Fe_3** with $CoCl_2$ and Hna. ICP-AES showed a Fe/Co ratio of 2.05, according well with the theoretical value of 2:1. In dilute HCl, **Fe_3-Co_2** can return to **Fe_3** (free of Co ions in the ICP-AES analysis), meaning that there is no Fe to Co exchange in the postsynthetic treatment. Single-crystal X-ray diffraction, X-ray photoelectron spectroscopy (XPS), and potentiometric titration also confirmed the successful installation of the $Co_2(na)_4(L^T)_2$ metalloligand (Figures 1c, S1c, S4, Scheme 1 and Tables S2, S3). It should be noted that, without addition of Hna, reaction of **Fe_3** with $CoCl_2{\cdot}6H_2O$ can give ion exchange products, such as $[Fe_2Co(\mu_3\text{-}O)(bdc)_3(L^T)_3]$ (Co:MCF-48 or **Co:Fe_3**).

We also tried to synthesize **Fe_3-Co_2** by direct solvothermal reaction using mixed Fe and Co salts as starting materials, but ICP-AES tests of the as-synthesized and partially acid-digested products showed that the Fe and Co ions are disorderly distributed, being similar to the ion exchange treatment of **Fe_3-Fe** (Table S1). On the other hand, $[\{Co_3(\mu_3\text{-}OH)(bdc)_3\}_4\{Co_2(na)_4(L^T)_2\}_3]$ (MCF-50 or **Co_3-Co_2**) isostructural with **Fe_3-Co_2** can be synthesized by using only Co salt as the metal source (Table S2 and Figures 1d and S1d). Scanning electron microscopy (SEM) images showed similar crystal sizes/morphologies for **Fe_3-Co_2**, **Fe_3**, **Fe_3-Fe**, and **Co:Fe_3** (Figure S5), further confirming that the postsynthetic modification processes occurred in the crystal-to-crystal manner.

The chemical stabilities of **Fe_3-Co_2**, **Fe_3**, **Fe_3-Fe**, **Co:Fe_3**, and **Co_3-Co_2** were checked in water at different pH values. As shown in Figure S6, **Fe_3-Co_2**, **Fe_3**, and **Fe_3-Fe** can remain intact at pH = 13 for at least 24 h, **Co:Fe_3** can maintain its framework for 1 h at pH = 13 or 24 h at pH = 12, whereas **Co_3-Co_2** collapses immediately even at pH = 7. These observations can be explained by the high chemical stability of the $Fe_3(\mu_3\text{-}O)(RCOO)_6(L^T)_3$ cluster. Further, thermogravimetry, PXRD, and CO_2 adsorption measurements showed that the target material **Fe_3-Co_2** can retain its open framework after guest removal (Figures S7−S10 and Table S4), being similar to **Fe_3-Fe**.[44] On the other hand, the intermediate compound **Fe_3** partially and irreversibly collapses after guest removal (Figures S8, S10 and Table S4). The very different thermal stabilities between **Fe_3-Fe**/**Fe_3-Co_2** and **Fe_3** is similar to their Ni analogues, which can be explained by the internal tension of the **flu-e** network and the cross-linking/stabilizing effects of tetradentate metalloligands.[44]

To test the electrocatalytic activity of **Fe_3-Co_2** for OER, linear sweep voltammetry (LSV) was performed in water at pH = 13 for **Fe_3-Co_2**@GC (microcrystalline sample coated on Glassy Carbon electrode with Nafion binder). As shown in Figures 2, S11 and S12, **Fe_3-Co_2**@GC displays very low onset potential of 1.46 V, overpotential of 283 mV at 10 mA cm^{-2}, and Tafel slope of 43 mV dec^{-1}. Considering the importance of electrode substrate on OER performances,[27,33] we also tested the OER performance of **Fe_3-Co_2** coated on Cu foam (**Fe_3-Co_2**@Cu) and Ni foam (**Fe_3-Co_2**@Ni). The onset potentials,

DOI: 10.1021/jacs.6b12353
J. Am. Chem. Soc. 2017, 139, 1778−1781

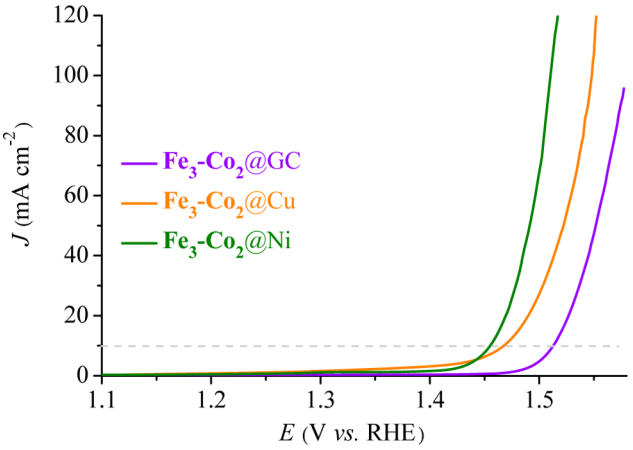

Figure 2. LSV curves of Fe_3-Co_2@GC, Fe_3-Co_2@Cu, and Fe_3-Co_2@Ni in water at pH = 13.

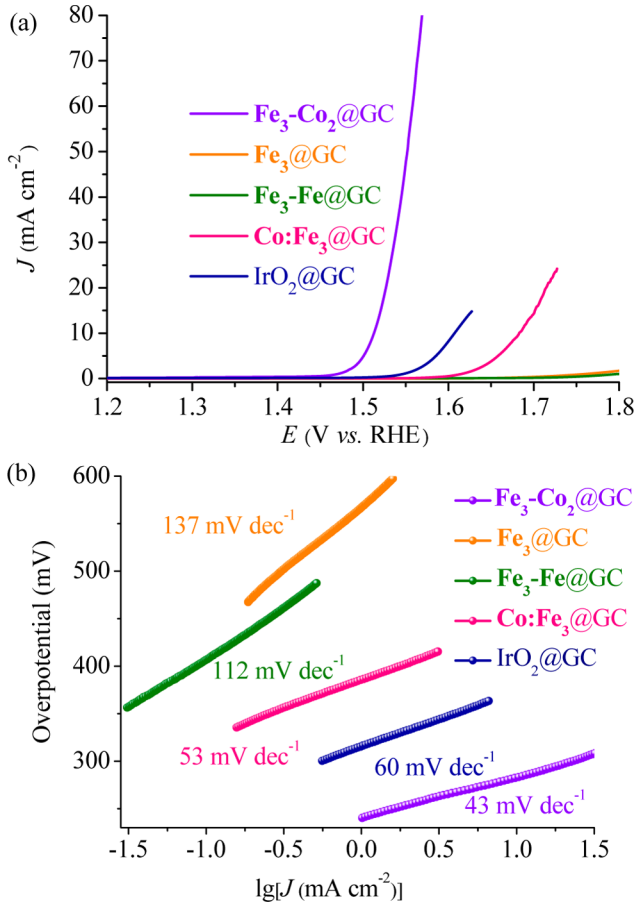

Figure 3. (a) LSV curves and (b) Tafel plots of Fe_3-Co_2@GC, Fe_3@GC, Fe_3-Fe@GC, Co:Fe_3@GC, and IrO_2@GC in water at pH = 13.

overpotentials (at 10 mA cm^{-2}), and Tafel slopes of Fe_3-Co_2@Cu/Fe_3-Co_2@Ni reach 1.43/1.42 V, 237/225 mV, and 79/48 mV dec^{-1}, respectively. The Faraday efficiency of Fe_3-Co_2@Ni for OER was measured to be virtually 100% (Figures S11 and S13), confirming that the observed electrochemical current was not originated from other side reactions. At the overpotential of 300 mV, the OER turnover frequencies (TOFs) at each Co ion of Fe_3-Co_2@GC, Fe_3-Co_2@Cu, and Fe_3-Co_2@Ni were calculated to be 0.27, 0.71, and 1.82 s^{-1}, respectively (Table S5). Similar with literature reports,[33,46] the Ni substrate also gives the best OER performance for Fe_3-Co_2. These OER performances are better than for almost all known catalysts (except Ni_3S_2@Ni) at the same condition (Table S5),[14,27−29,33,46] and even many catalysts working in water at pH = 14 (Table S6).[1,14−17,26,27] In contrast, Fe_3, Fe_3-Fe, and Co:Fe_3 showed very poor electrocatalytic OER performances at the same condition (Figures 3 and S14−16).

To compare the OER activities of Fe_3-Co_2 and Co_3-Co_2, LSV curves of relevant MOFs were measured in 4:1 CH_3CN/PB (PB = phosphate buffer water solution at pH = 7). As shown in Figure S17, the OER performances of Fe_3-Co_2@GC and Co_3-Co_2@GC are very similar, which are much better than those of Fe_3@GC, Fe_3-Fe@GC, and Co:Fe_3@GC, consistent with the trends observed in alkaline water at pH = 13. Considering the usefulness of electrocatalytic OER in neutral water,[8] LSV curve of Fe_3-Co_2@GC was also measured in water at pH = 7 (Figure S18), which displays onset potential of 1.53 V, overpotential of 431 mV at 2 mA cm^{-2}, Tafel slope of 134 mV dec^{-1}, and TOF of 0.132 s^{-1} at 400 mV overpotential, which are all the best values among known catalysts (Table S7).[8,27,47] At the same condition, $[Co_2(dobdc)(H_2O)_2]$ (MOF-74-Co, H_2dobdc = 2,5-dihydroxyterephthalic acid) with square-pyramidal (without H_2O ligand) or octahedral (with H_2O ligand) Co ions and $[Co(mim)_2]$ (ZIF-67, Hmim = 2-methylimidazole) with tetrahedral (without H_2O ligand) Co ions display much lower OER performances (Figures S18−19 and Table S7). These observations proved the special coordination mode of Co ions in the paddle-wheel type dicobalt carboxylate clusters is the key for achieving the supreme OER activities. Fe_3-Co_2 also exhibits high stability in OER processes in water at both pH = 13 and pH = 7. Negligible changes of LSV, PXRD, XPS, MS, and SEM were observed after catalysis operations for 24 h (Figures S20−21). Nevertheless, Fe_3-Co_2 completely collapses after OER test for 96 h (Figure S22), demonstrating that its OER activity is originated from the structures of its open framework and the dicobalt clusters.

In summary, by using a modular synthesis method involving two-step, single-crystal to single-crystal, postsynthetic modification, we successfully immobilized the paddle-wheel type cobalt carboxylate cluster in a unique Fe(III) dicarboxlyalte framework, and achieved exceptionally high OER catalytic activities. These results should be insightful for future design and synthesis of new MOF catalysts.

■ ASSOCIATED CONTENT

Supporting Information

The Supporting Information is available free of charge on the ACS Publications website at DOI: 10.1021/jacs.6b12353.

Experimental details, additional figures/tables (PDF)
X-ray crystallographic files (CIF)

■ AUTHOR INFORMATION

Corresponding Authors

*liaopq3@mail.sysu.edu.cn
*zhangjp7@mail.sysu.edu.cn

ORCID

Jie-Peng Zhang: 0000-0002-2614-2774

Notes

The authors declare no competing financial interest.

DOI: 10.1021/jacs.6b12353
J. Am. Chem. Soc. 2017, 139, 1778−1781

■ ACKNOWLEDGMENTS

This work was supported by the "973 Project" (2014CB845602) and NSFC (21225105, 21290173, and 21473260).

■ REFERENCES

(1) Jiao, Y.; Zheng, Y.; Jaroniec, M.; Qiao, S.-Z. *Chem. Soc. Rev.* **2015**, *44*, 2060.
(2) Xia, B.-Y.; Yan, Y.; Li, N.; Wu, H.-B.; Lou, X.-W.; Wang, X.-C. *Nat. Energy* **2016**, *1*, 15006.
(3) Gao, X.-H.; Zhang, H.-X.; Li, Q.-G.; Yu, X.-G.; Hong, Z.-L.; Zhang, X.-W.; Liang, C.-D.; Lin, Z. *Angew. Chem., Int. Ed.* **2016**, *55*, 6290.
(4) Jin, Y.-S.; Wang, H.-T.; Li, J.; Yue, X.; Han, Y.-J.; Shen, P.-K.; Cui, Y. *Adv. Mater.* **2016**, *28*, 3785.
(5) Chen, D.-J.; Chen, C.; Baiyee, Z. M.; Shao, Z.-P.; Ciucci, F. *Chem. Rev.* **2015**, *115*, 9869.
(6) Li, Y.-G.; Dai, H.-J. *Chem. Soc. Rev.* **2014**, *43*, 5257.
(7) Minguzzi, A.; Fan, F.-R. F.; Vertova, A.; Rondinini, S.; Bard, A. J. *Chem. Sci.* **2012**, *3*, 217.
(8) Kanan, M. W.; Nocera, D. G. *Science* **2008**, *321*, 1072.
(9) Ling, T.; Yan, D.-Y.; Jiao, Y.; Wang, H.; Zheng, Y.; Zheng, X.-L.; Mao, J.; Du, X.-W.; Hu, Z.-P.; Jaroniec, M.; Qiao, S.-Z. *Nat. Commun.* **2016**, *7*, 12876.
(10) Chen, S.; Qiao, S.-Z. *ACS Nano* **2013**, *7*, 10190.
(11) Zhu, Y.-P.; Ma, T.-Y.; Jaroniec, M.; Qiao, S.-Z. *Angew. Chem., Int. Ed.* **2017**, *56*, 1324.
(12) Meng, C.; Ling, T.; Ma, T.-Y.; Wang, H.; Hu, Z.-P.; Zhou, Y.; Mao, J.; Du, X.-W.; Jaroniec, M.; Qiao, S.-Z. *Adv. Mater.* **2016**, 1604607.
(13) Yin, Q.; Tan, J. M.; Besson, C.; Geletii, Y. V.; Musaev, D. G.; Kuznetsov, A. E.; Luo, Z.; Hardcastle, K. I.; Hill, C. L. *Science* **2010**, *328*, 342.
(14) Ma, T.-Y.; Dai, S.; Jaroniec, M.; Qiao, S.-Z. *J. Am. Chem. Soc.* **2014**, *136*, 13925.
(15) Hu, H.; Guan, B.-Y.; Xia, B.-Y.; Lou, X.-W. *J. Am. Chem. Soc.* **2015**, *137*, 5590.
(16) Jin, H.-Y.; Wang, J.; Su, D.-F.; Wei, Z.-Z.; Pang, Z.-F.; Wang, Y. *J. Am. Chem. Soc.* **2015**, *137*, 2688.
(17) Zhang, Y.-Q.; Ouyang, B.; Xu, J.; Jia, G.-C.; Chen, S.; Rawat, R. S.; Fan, H.-J. *Angew. Chem., Int. Ed.* **2016**, *55*, 8670.
(18) He, Y.-B.; Zhou, W.; Qian, G.-D.; Chen, B.-L. *Chem. Soc. Rev.* **2014**, *43*, 5657.
(19) Qiu, S.-L.; Xue, M.; Zhu, G.-S. *Chem. Soc. Rev.* **2014**, *43*, 6116.
(20) Xiao, D. J.; Oktawiec, J.; Milner, P. J.; Long, J. R. *J. Am. Chem. Soc.* **2016**, *138*, 14371.
(21) Qin, J.-S.; Du, D.-Y.; Guan, W.; Bo, X.-J.; Li, Y.-F.; Guo, L.-P.; Su, Z.-M.; Wang, Y.-Y.; Lan, Y.-Q.; Zhou, H.-C. *J. Am. Chem. Soc.* **2015**, *137*, 7169.
(22) Kornienko, N.; Zhao, Y.-B.; Kley, C. S.; Zhu, C.-H.; Kim, D.; Lin, S.; Chang, C. J.; Yaghi, O. M.; Yang, P.-D. *J. Am. Chem. Soc.* **2015**, *137*, 14129.
(23) Inukai, M.; Horike, S.; Itakura, T.; Shinozaki, R.; Ogiwara, N.; Umeyama, D.; Nagarkar, S.; Nishiyama, Y.; Malon, M.; Hayashi, A.; Ohhara, T.; Kiyanagi, R.; Kitagawa, S. *J. Am. Chem. Soc.* **2016**, *138*, 8505.
(24) Sheberla, D.; Bachman, J. C.; Elias, J. S.; Sun, C.-J.; Shao-Horn, Y.; Dincă, M. *Nat. Mater.* **2017**, *16*, 220.
(25) Miner, E. M.; Fukushima, T.; Sheberla, D.; Sun, L.; Surendranath, Y.; Dincă, M. *Nat. Commun.* **2016**, *7*, 10942.
(26) Zhao, S.-L.; Wang, Y.; Dong, J.-C.; He, C.-T.; Yin, H.-J.; An, P.-F.; Zhao, K.; Zhang, X.-F.; Gao, C.; Zhang, L.-J.; Lv, J.-W.; Wang, J.-X.; Zhang, J.-Q.; Khattak, A. M.; Khan, N. A.; Wei, Z.-X.; Zhang, J.; Liu, S.-Q.; Zhao, H.-J.; Tang, Z.-Y. *Nat. Energy* **2016**, *1*, 16184.
(27) Lu, X.-F.; Liao, P.-Q.; Wang, J.-W.; Wu, J.-X.; Chen, X.-W.; He, C.-T.; Zhang, J.-P.; Li, G.-R.; Chen, X.-M. *J. Am. Chem. Soc.* **2016**, *138*, 8336.
(28) Manna, P.; Debgupta, J.; Bose, S.; Das, S. K. *Angew. Chem., Int. Ed.* **2016**, *55*, 2425.
(29) Wang, S.-B.; Hou, Y.-D.; Lin, S.; Wang, X.-C. *Nanoscale* **2014**, *6*, 9930.
(30) Tan, K.; Nijem, N.; Canepa, P.; Gong, Q.-H.; Li, J.; Thonhauser, T.; Chabal, Y. J. *Chem. Mater.* **2012**, *24*, 3153.
(31) Chui, S. S. Y.; Lo, S. M. F.; Charmant, J. P. H.; Orpen, A. G.; Williams, I. D. *Science* **1999**, *283*, 1148.
(32) Wade, C. R.; Dinca, M. *Dalton Trans.* **2012**, *41*, 7931.
(33) Wang, L.; Wu, Y.-Z.; Cao, R.; Ren, L.-T.; Chen, M.-X.; Feng, X.; Zhou, J.-W.; Wang, B. *ACS Appl. Mater. Interfaces* **2016**, *8*, 16736.
(34) Feldblyum, J. I.; Liu, M.; Gidley, D. W.; Matzger, A. J. *J. Am. Chem. Soc.* **2011**, *133*, 18257.
(35) Zhang, Z.-J.; Zhang, L.-P.; Wojtas, L.; Eddaoudi, M.; Zaworotko, M. J. *J. Am. Chem. Soc.* **2012**, *134*, 928.
(36) Wang, K.-C.; Feng, D.-W.; Liu, T.-F.; Su, J.; Yuan, S.; Chen, Y.-P.; Bosch, M.; Zou, X.-D.; Zhou, H.-C. *J. Am. Chem. Soc.* **2014**, *136*, 13983.
(37) Zhang, W.; Hu, Y.-L.; Ge, J.; Jiang, H.-L.; Yu, S.-H. *J. Am. Chem. Soc.* **2014**, *136*, 16978.
(38) Férey, G.; Mellot-Draznieks, C.; Serre, C.; Millange, F.; Dutour, J.; Surblé, S.; Margiolaki, I. *Science* **2005**, *309*, 2040.
(39) Serre, C.; Mellot-Draznieks, C.; Surblé, S.; Audebrand, N.; Filinchuk, Y.; Férey, G. *Science* **2007**, *315*, 1828.
(40) Lee, S.; Kapustin, E. A.; Yaghi, O. M. *Science* **2016**, *353*, 808.
(41) Wei, Y.-S.; Zhang, M.; Liao, P.-Q.; Lin, R.-B.; Li, T.-Y.; Shao, G.; Zhang, J.-P.; Chen, X.-M. *Nat. Commun.* **2015**, *6*, 8348.
(42) Talin, A. A.; Centrone, A.; Ford, A. C.; Foster, M. E.; Stavila, V.; Haney, P.; Kinney, R. A.; Szalai, V.; El Gabaly, F.; Yoon, H. P.; Léonard, F.; Allendorf, M. D. *Science* **2014**, *343*, 66.
(43) Zheng, S.-T.; Zhao, X.; Lau, S.; Fuhr, A.; Feng, P.-Y.; Bu, X.-H. *J. Am. Chem. Soc.* **2013**, *135*, 10270.
(44) Wei, Y.-S.; Shen, J.-Q.; Liao, P.-Q.; Xue, W.; Zhang, J.-P.; Chen, X.-M. *Dalton Trans.* **2016**, *45*, 4269.
(45) Mellot-Draznieks, C.; Dutour, J.; Férey, G. *Z. Anorg. Allg. Chem.* **2004**, *630*, 2599.
(46) Zhou, W.-J.; Wu, X.-J.; Cao, X.-H.; Huang, X.; Tan, C.-L.; Tian, J.; Liu, H.; Wang, J.-Y.; Zhang, H. *Energy Environ. Sci.* **2013**, *6*, 2921.
(47) Wu, Y.-Z.; Chen, M.-X.; Han, Y.-Z.; Luo, H.-X.; Su, X.-J.; Zhang, M.-T.; Lin, X.-H.; Sun, J.-L.; Wang, L.; Deng, L.; Zhang, W.; Cao, R. *Angew. Chem., Int. Ed.* **2015**, *54*, 4870.

DOI: 10.1021/jacs.6b12353
J. Am. Chem. Soc. 2017, 139, 1778−1781